ISSN 1330–0016
CODEN FIZBE7

# WEAK ABSORPTION AND RESONANCES IN LIGHT HEAVY-ION REACTIONS INDUCED BY THE NON-$\alpha$-TYPE $^{14}$C NUCLEUS

SUZANA SZILNER[a,b,1], FLORENT HAAS[b] and ZORAN BASRAK[a]

[a]*Ruđer Bošković Institute, HR-10 002 Zagreb, Croatia*

[b]*Institut de Recherches Subatomiques, CNRS-IN2P3/ULP, Strasbourg, France*

**Paper devoted to honour the memory of Professor Nikola Cindro**

Received 28 January 2003; revised manuscript received 19 March 2003
Accepted 15 September 2003 Online 3 March 2004

The observation of resonant structures attributed to nuclear molecular configurations in $\alpha$-type systems involving the $^{12}$C and $^{16}$O nuclei is a clear signature of a weak and surface-transparent absorption in these light heavy-ion reactions at energies around and up to well above the Coulomb barrier. Such a weak absorption, i.e. nuclear-surface transparency, is also predicted in reactions induced by the $^{14}$C nucleus owing to the very special structure of low-lying states of this non-$\alpha$-type nucleus. The experimental search for resonant structures in the $^{14}\mathrm{C}+{}^{14}\mathrm{C}$, $^{14}\mathrm{C}+{}^{12}\mathrm{C}$ and $^{14}\mathrm{C}+{}^{16}\mathrm{O}$ reactions undertaken by the Strasbourg–Zagreb collaboration is described and discussed in the context of weak-absorption phenomena. Strong and correlated resonances have been observed in the three systems studied and particularly in those decay channels which are sensitive to the largest partial waves in the entrance channel. As the incident energy increases, weak and surface-transparent absorption gives rise to refractive effects, i.e to the nuclear rainbow. Indeed, nuclear rainbows have been observed recently in the same $\alpha$-type $^{12}\mathrm{C}+{}^{12}\mathrm{C}$, $^{12}\mathrm{C}+{}^{16}\mathrm{O}$ and $^{16}\mathrm{O}+{}^{16}\mathrm{O}$ systems in which prominent nuclear molecular resonances have been reported at lower energies. It is predicted that such refractive effects should also be observed in the $^{14}$C-induced reactions at energies above $\sim 5$ MeV per nucleon.

PACS numbers: 25.70.Bc, 25.70.Ef, 25.70.-z UDC 539.17

Keywords: heavy ions, $^{14}$C radioactive beam, $^{14}$C targets, molecular resonances, refractive effects, nuclear rainbow

[1]Present address: Istituto Nazionale di Fisica Nucleare, Laboratori Nazionali di Legnaro, I-35020 Legnaro (PD), Italy

## 1. Introduction

The interaction between heavy ions is usually dominated by a strong absorption which leads to the formation of a compound nucleus. However, the exciting and unexpected results from the first measurements with heavy ions in electrostatic tandem accelerators pointed to an exception to this rule [1]. The reported intermediate structures in the excitation functions of the elastic and reaction channels of the $^{12}C+^{12}C$ collision near the Coulomb barrier have been demonstrated to be genuine quantum mechanical states (resonances) of the system. A dumb-bell-like $^{12}C-^{12}C$-cluster configuration was attributed to these states and they were named nuclear molecules. Until now, resonance phenomena have been reported in various light heavy-ion systems for a wide range of incident energy. Different models have been developed to describe resonant structures [2, 3]. With increasing incident energy, the interaction time decreases and the width of the structures increases. Above a certain energy (about 5 MeV per nucleon) the broad structures are generally no longer correlated in the different reaction channels as the genuine resonant phenomena are. In the scattering channel, these structures are explained through the interference phenomena which are of diffractive nature at forward angles and refractive (nuclear rainbow and associated Airy oscillations [4]) at backward angles.

Nuclear molecular configurations are the most prominent examples of clustering phenomena in nuclear physics. The reaction partners with non-negligible probability conserve their identity for a short period of time. Qualitatively, they can be described as a system of an elongated shape (extreme deformation) made of a touching configuration of the target and projectile nuclei orbiting around the common centre of mass. This picture implies a certain degree of nuclear-surface transparency which ensures the ("covalent") surface binding of the system and prevents its prompt collapsing into a compound nucleus. On the other hand, rainbow scattering appears when the nuclear potential is strong and when the absorption is incomplete. The existence of nuclear rainbow speaks in favour of deeply penetrating partial waves, which in the region of overlap of the two interacting nuclei produce a nuclear density of twice the normal value. A remarkable fact is that the strong resonant structure and the nuclear rainbow have been observed in the same systems at different bombarding energies. The common feature of these systems is a certain 'transparency' of the interaction which is a signature of weak absorption. The study of both the resonant and refractive behaviour can be considered as a probe of the properties of nuclei under extreme conditions, where the reduced absorption is crucial for their observability.

In this paper, we present an overview of two predictive models of molecular resonances (Sect. 2) and experimental results on $^{14}C$-induced resonant (Sect. 3) and refractive reactions (Sect. 4) carried out by the Strasbourg and Zagreb groups. In Sect. 5, we discuss technical particularities of radioactive $^{14}C$ beams and targets, while in Sect. 6 we give the conclusion.

## 2. Weak absorption in light heavy-ion reactions

A few attempts have been made to understand the underlying physical background of the above discussed reduced absorption in certain nuclear systems and, in particular, to predict in which systems the observation of molecular states (and recently nuclear rainbows) could be expected? Here we are going to briefly discuss only two models which were developed in Zagreb and Strasbourg, respectively, which are reputed by their good predictive power of the observability of resonant phenomena: the orbiting cluster model (OCM) [5] and the number of open channels (NOC) calculations [6, 7]. They are both based on simple principles of the formal theory of intermediate-width states, i.e., on a concept of doorway states whose total width consists of two components: the spreading and escape widths [8]. The necessary condition for a doorway state not to dump down its strength into the surrounding continuum is that the spreading width should not be too large. Similarly, the probability for a doorway state to directly decay into open channels should not be large either, i.e., the escape width should be small, too. The spreading width is proportional to the compound-nucleus level density and these features are studied within the OCM, while the escape width is proportional to the number of open reaction channels and the study of these features is emphasized within the NOC calculation.

In the OCM, the interacting system is approximated by a rigid rotator consisting of two touching spherical nuclei. It has a characteristic energy spectrum which forms a rotational molecular band, as in molecular physics. The band members or resonant states can be observed if their excitation energies ($E^*$) and spins ($J$) lie in the so-called molecular window [9], a region of the $(E^*, J)$ space of the corresponding compound-nucleus within which the level density is small and relatively constant. A small compound-nucleus-level density means a small spreading width which ensures the weak absorption within the molecular window. Owing to the known relatively low level density of the so-called $\alpha$-type nuclei, the OCM predicts [5] that resonant phenomena should be strongest for reactions involving $^{12}$C and $^{16}$O nuclei. The prediction of resonance observability is made by comparing the spreading width of a given system to the width of the $^{12}\text{C} + ^{12}\text{C}$ system. These predictions are in perfect agreement with experimental results. Indeed, the strongest resonances are observed in the $^{12}\text{C} + ^{12}\text{C}$, $^{12}\text{C} + ^{16}\text{O}$ and $^{16}\text{O} + ^{16}\text{O}$ reactions. Besides the above systems, the model predicts a dozen of other candidate-systems for resonant behaviour including the $^{14}\text{C} + ^{14}\text{C}$ and $^{14}\text{C} + ^{16}\text{O}$ systems, but not the $^{12}\text{C} + ^{14}\text{C}$ system [10].

The NOC calculation implicitly takes into account the contribution of the spreading width by accounting for the saturation of the fusion cross section of light heavy-ion reactions caused by the existence of a critical angular momentum for fusion. On the other hand, it explicitly accounts for the escape width by enumerating the direct reaction channels which progressively open as the incident energy increases. Thus, at higher incident energies, weak absorption arises mainly from the small number of open direct reaction channels which involve the most peripheral incident partial waves close to the grazing angular momentum, $L_{\text{g}}$. For a given system, NOC is obtained by a triple summation over all possible two-body exit channels (mass partitions, angular momentum couplings and energy repartitions; for more details, see Refs. [6] and [7]). The result of the NOC calculation for the entrance channel composed of even-even carbon and oxygen isotopes is displayed in Fig. 1 as a function of $L_{\text{g}}$. The calculation covers a large range of incident

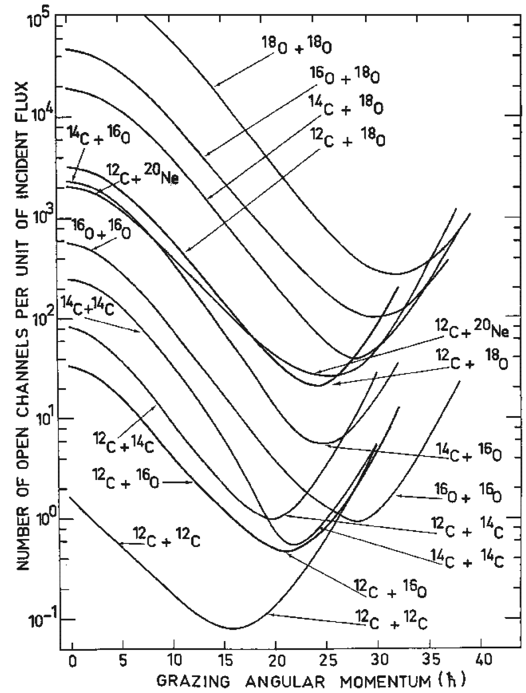

*Fig. 1. Calculated NOC for the reactions involving even-even isotopes of carbon and oxygen nuclei [6].*

energies above the Coulomb barrier at which $L_g = 0$. The $^{12}$C + $^{12}$C system is an extreme case: NOC is small over a wide range of $L_g$. This is consistent with an exceptionally weak absorption and the resulting prominent resonant behaviour and rainbow phenomena observed in this system. The $^{12}$C + $^{16}$O and $^{16}$O + $^{16}$O systems, composed of $\alpha$-type nuclei, also have small NOC minima, i.e. weak absorption, in agreement with the OCM predictions. What is remarkable in the NOC calculation is the strikingly small NOC minima values for the $^{12}$C + $^{14}$C, $^{14}$C + $^{14}$C and $^{14}$C + $^{16}$O reactions. Although $^{14}$C is not an $\alpha$-type nucleus, it has a closed neutron shell and a closed proton sub-shell. Thus, it displays a large energy gap ($E > 6.0$ MeV) between the ground state and the first excited state. In this sense, $^{14}$C 'resembles' the closed-shell nucleus $^{16}$O and the $L_g$ vs. NOC curves (values and variations) for the $^{12}$C + $^{14}$C and $^{14}$C + $^{14}$C systems are very similar to those for the $^{12}$C + $^{16}$O and $^{16}$O + $^{16}$O systems, respectively. These NOC predictions for the systems involving the $^{14}$C nucleus were our main motivation to undergo an experimental programme of search for resonant structures in the $^{14}$C + $^{14}$C, $^{12}$C + $^{14}$C and $^{14}$C + $^{16}$O reactions.

## 3. $^{14}$C-*induced reactions: resonant features*

In this section we present the experimental methods and results of a study undertaken by the Strasbourg group on the $^{14}$C + $^{14}$C, $^{12}$C + $^{14}$C and $^{14}$C + $^{16}$O reactions. Most of the experiments have been carried out in collaboration with the Zagreb group of Prof. Nikola Cindro.

### 3.1. Experimental methods

The measurements using radioactive $^{14}$C beams and targets were performed at the electrostatic tandem accelerators in Munich and Strasbourg. The targets and pellets (used in the accelerator ion source) were prepared in the Munich target laboratory, which was especially equipped to handle radioactive material. Details on the beam production and the targets used can be found in Ref. [11] and in Refs. [11] and [12], respectively. A search for resonant structures requires measurements of the reaction-product excitation functions over a wide range of incident energies in small energy steps for which the tandem accelerators are ideally suited. Two experimental techniques were used: the $\gamma$-ray method (GRM) and the kinematical-coincidence method (KCM).

In GRM, the reaction products (fusion evaporation residues and fragments from direct reactions) are identified through their characteristic $\gamma$ rays detected in large volume Ge(Li) detectors. The observed $\gamma$ rays correspond generally to transitions between low-lying states and their intensities are measured as a function of incident energy. The GRM is an 'inclusive' method which allows to obtain angle-integrated excitation functions for the main reaction channels over a wide energy range during a limited beam time.

In KCM, the binary reaction products (essentially fragments from direct reactions) are detected in coincidence and their masses are identified by fragment energies and angles of impact onto two large area position-sensitive Si detectors. The Si detectors were placed at relatively large angles ($\theta_{\mathrm{c.m.}} > 40°$) to enhance the yields of binary channels produced by mechanisms with long interacting time (like the formation of molecular states) compared with forward-peaked binary channels from more direct reactions. KCM is an 'exclusive' method which allows to obtain angular distributions and partially angle-integrated excitation functions of the strongest binary reaction channels. Of course, KCM is more beam time consuming than GRM. Thus, for the three reactions under study, the complete excitation functions were first measured using GRM and then, in limited incident energy regions of interest, angular distributions were measured for the binary channels using KCM to obtain the characteristics of the resonant structures (decay widths and spins). Details on the two experimental techniques used can be found in Refs. [11], [12] and [13] for GRM and in Refs. [14], [15] and [16] for KCM.

### 3.2. Results and discussion

#### 3.2.1. The $^{14}$C + $^{14}$C reaction

For the $^{14}$C + $^{14}$C system, the first measurements of the elastic scattering were reported at the same time by the Munich [18] and the Los Alamos [19] groups. N. Cindro was the driving spirit of the Los Alamos experiment.

The excitation function obtained at 90°, measured at $E_{\mathrm{c.m.}} = 6$ to 35 MeV, is plotted in Fig. 2. It shows the pronounced and regular oscillatory behaviour similar to the one observed in the $^{16}\mathrm{O} + ^{16}\mathrm{O}$ scattering. The width of the observed gross structures is about 3 MeV, with peak-to-valley ratios larger than one order of magnitude. The pattern of the angular distributions measured at energies corresponding to the maxima of the excitation function is consistent with the contribution of one dominant angular momentum, i.e., these structures are states of definite spin: the resonances.

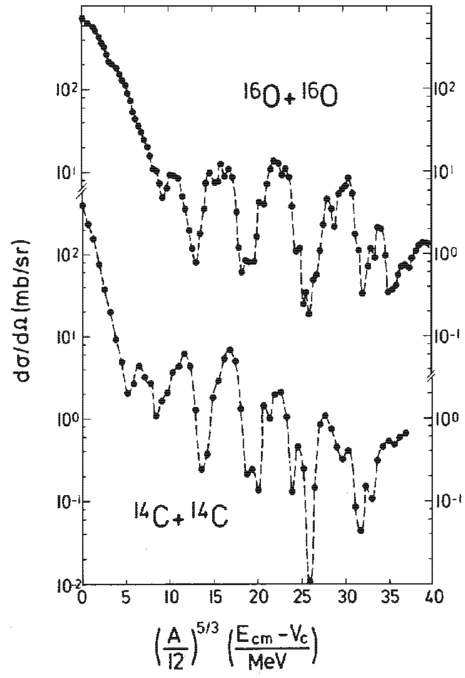


*Fig. 2. Comparison of the* 90° *elastic excitation functions of the* $^{16}\mathrm{O} + ^{16}\mathrm{O}$ *and* $^{14}\mathrm{C} + ^{14}\mathrm{C}$ *reactions [20]. The scale on the abscissa is proportional to the square of the grazing angular momentum at a given centre-of-mass energy with the aim to correct for the different masses and atomic numbers of the two systems.*

The reaction channels of the $^{14}\mathrm{C} + ^{14}\mathrm{C}$ collision were studied using GRM [12] to determine whether the structure observed in the elastic scattering also shows up in the reaction channels. The results are plotted in Fig. 3 (top-left panel). The measurement was performed from $E_{\mathrm{c.m.}}$=12 to 32 MeV in small energy steps. In the strongest fusion-evaporation channels leading to the Ne isotopes, structures are clearly visible. In particular, the excitation function of the $^{22}\mathrm{Ne}$ $(\alpha 2n)$ evaporation channel is very similar to the one reported by the Strasbourg group for the $^{24}\mathrm{Mg}$ $(2\alpha)$ channel in $^{16}\mathrm{O} + ^{16}\mathrm{O}$ [21]. Structures are connected with the highest angular momenta brought into the system. Thus, they are observed in the fusion-evaporation channels sensitive to such momenta, i.e., the $\alpha$ channels (Ne isotopes)

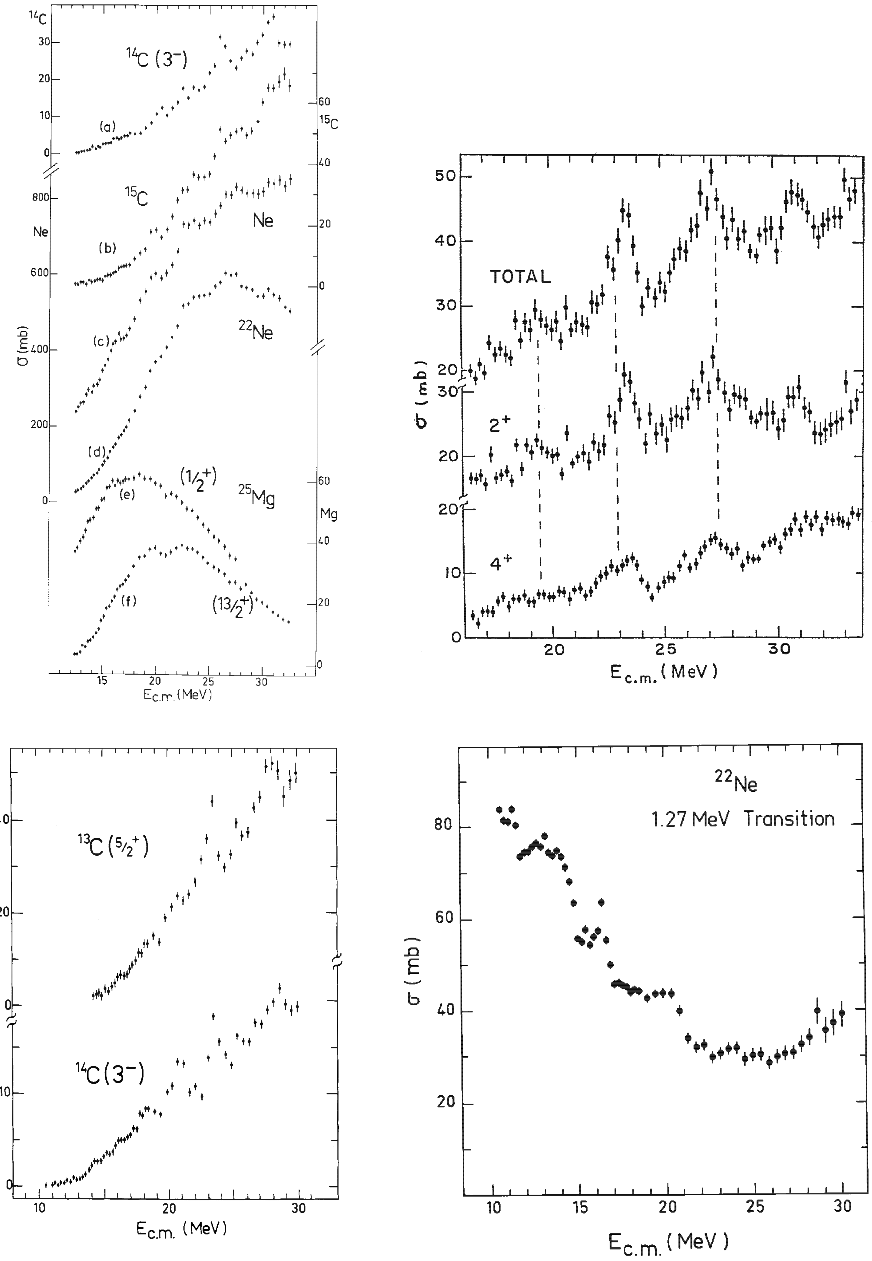


*Fig. 3. Excitation functions obtained using GRM. Top-left: Reaction $^{14}$C + $^{14}$C [12]: the inelastic ($^{14}$C), transfer ($^{15}$C) and fusion-evaporation (Ne and Mg) channels. Top-right: Reaction $^{14}$C + $^{16}$O [14]: the transfer channels to states of $^{18}$O. Bottom-left and -right: Reaction $^{12}$C + $^{14}$C [13]: the inelastic ($^{14}$C), transfer ($^{13}$C) and α-fusion-evaporation ($^{22}$Ne) channels.*

and the $^{25}$Mg (3n) channel feeding a high spin state. The excitation functions of the two binary reaction channels which could be extracted (inelastic to $^{14}$C($3^-$) and one neutron transfer to $^{15}$C) also show strong structure which is correlated in energy between them and with fusion channels.

One should note that strong resonant structure has been observed using GRM in the feeding of the $3^-$ states in the $^{14}$C ($E_x$=6.73 MeV) and $^{16}$O ($E_x$=6.13 MeV) through the $^{14}$C+$^{14}$C [12] and $^{16}$O+$^{16}$O [21] reactions, respectively. These two states are deformed particle-hole states. Thus, they are preferentially populated in the decay of the strongly deformed molecular states. For example, a structure of two neutrons coupled to the ground state of $^{12}$C [22], described by the $^{12}\mathrm{C}\otimes p_{1/2} \otimes d_{5/2}$ configuration, is attributed to the $3^-$ state in $^{14}$C. This state is known to have the largest collective deformation parameter among all known $^{14}$C states [23].

The energy dependence of the cross sections of binary reaction channels differs from the bell-shaped excitation functions of the fusion channels. The yields of the binary channels rise steadily in the region where the total fusion cross section begins to saturate. Such an energy dependence of the cross sections underlines the importance of inelastic excitations and transfer reactions in the energy region well above the Coulomb barrier. As the energy increases, the cross section of the fusion channels decreases, whereas the inelastic and transfer channels continue to rise and the absorption in these channels grows gradually, especially for incident angular momenta close to grazing ($L_g$). The oscillatory structure appearing in several channels of $^{14}$C+$^{14}$C closely resembles the situation in $^{16}$O+$^{16}$O (see Figs. 2 and 3). Thus, a common origin of the observed gross structures is required. As mentioned before, both in $^{16}$O and $^{14}$C nuclei, there is a large energy gap between the ground and first excited state. As the energy increases, the absorption due to inelastic processes becomes relevant but remains small owing to the large energy gap in both nuclei, as predicted by the NOC calculations. The resonant structures in both systems are very similar. This can be attributed to the similarity of the low-excitation-energy nuclear structures of these nuclei despite of the fact that the $^{14}$C is not an $\alpha$-type nucleus.

### *3.2.2.* The $^{12}$C+$^{14}$C reaction

A $^{14}$C-beam ranging between $E_{\mathrm{c.m.}}$=18.5 and 26.3 MeV in small energy steps was used in a GRM study of the $^{12}$C+$^{14}$C reaction [13]. These energies correspond to a range where strong structure was found in the $^{12}$C+$^{16}$O reaction. Figure 3 (bottom-left panel) shows that strong structure was again observed in the inelastic scattering to the $^{14}$C($3^-$) state and in the one-neutron transfer channel to the $^{13}$C($5/2^+$) state. Strong resonances correlated in both channels were observed at $E_{\mathrm{c.m.}}$=20.7, 23.5 and 27.5 MeV with a width of approximately 1.5 MeV and peak-to-valley ratios of about 2:1. The observed structure was rather weak in the excitation functions of the fusion-evaporation channels which constitute the main part of the reaction cross section. An exception was the $\alpha$-channel feeding the $^{22}$Ne nucleus (see the bottom-right panel in Fig. 3). In this channel, pronounced and narrow structure was observed at $E_{\mathrm{c.m.}} < 20$ MeV and was very similar to the results reported in GRM studies of the $\alpha$-fusion-evaporation channels of the $^{12}C+^{12}C$ [24] and $^{12}C+^{16}O$ [25] reactions. It is rather unfortunate that the $^{22}Ne$ excitation function could not be extended to lower energies because it seems that the $^{12}C+^{14}C$ reaction shows resonances in the $\alpha$-fusion-evaporation channels even at energies close to the Coulomb barrier, as in the case of the $^{12}C+^{12}C$ and $^{12}C+^{16}O$ reactions. Strong resonances in the binary-reaction channels and in the $\alpha$-fusion-evaporation channels are in good agreement with the NOC assumption that they are connected with the highest angular momenta brought into the system.

The $^{14}C+^{12}C$ reaction was also studied using KCM at 13 incident energies ranging from $E_{c.m.}$=19.4 to 24.9 MeV [16]. In this energy range, the resonances observed at $E_{c.m.}$=20.7 and 23.5 MeV were seen using both experimental techniques (GRM and KCM). Using KCM, they were observed in the large-angle elastic scattering data, and the corresponding angular distributions could be analysed. The on-resonance angular distributions are in good agreement with a dominant $L$=16 partial wave for the resonance at $E_{c.m.}$=20.7 and with $L$ =18 for the $E_{c.m.}$ =23.5 resonance. In the left panel of Fig. 4, the resonant yield of the $^{14}C(3^-)$ inelastic channel is plotted together with the proposed $^{12}C-^{14}C$ highly deformed molecular band. At a given incident energy, such resonating partial waves have significantly higher angular momenta than the grazing partial waves. This is in agreement with the picture of two carbon nuclei orbiting around each other and exchanging one or two neutrons at distances well outside the strong interaction radius. In this case, the resonant process is strongly related with the neutron rearrangement mechanism.

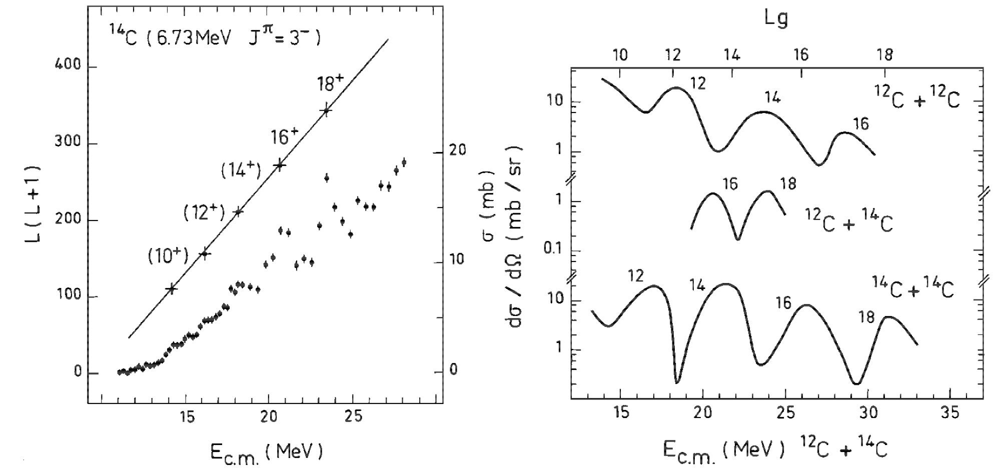


*Fig. 4. Left panel: The excitation function (obtained using GRM) of the* $^{14}C(3^- \rightarrow 0^+)$ *$\gamma$-transition excited in the* $^{12}C+^{14}C$ *reaction [13] together with the proposed high-moment-of-inertia molecular band [16]. Note the unusual (swapped) abscissae and ordinate axes of the band. Right panel: The 90° elastic excitation functions showing the gross structure of the* $^{12}C+^{12}C$ *[26],* $^{12}C+^{14}C$ *[16] and* $^{14}C+^{14}C$ *[19] reactions. The energy scale applies to* $^{14}C+^{12}C$ *and has been modified for the other two systems to match the grazing angular momenta (see Ref. [16]).*

In the right panel of Fig. 4, the 90° elastic excitation functions are compared for the $^{12}$C + $^{14}$C [16] and the identical boson systems $^{12}$C + $^{12}$C [15, 26] and $^{14}$C + $^{14}$C [19]. In the two latter systems, the gross structure is similar and arises essentially from the grazing waves which are weakly absorbed. In both systems, the partial waves are close to $L_g$, while in $^{12}$C + $^{14}$C, the dominant angular momenta are by about 3 units larger than $L_g$. This situation can be explained by the very negative $Q$-value needed for neutron rearrangements in the two identical boson systems, while most of the outgoing flux of the $^{12}$C + $^{14}$C reaction is in the one- and two-neutron transfer channels. These two channels involve the rearrangement of neutrons at distances where only the tails of the nuclear densities overlap. Such a picture suggests molecular configurations which are held together by orbiting (sharing) of the valence neutrons.

Furthermore, the symmetry of the system composed of two identical cores bound by a pair of neutrons would explain the absence of the odd members in the proposed moment-of-inertia molecular band (see Fig. 4). The occurrence of resonances with an even-L sequence results from the parity dependence of the nucleus-nucleus potential discussed in Ref. [27]. This effect is known to be important in collisions between light heavy ions with similar masses and is particularly strong at backward angles. Any attempt to explain the resonances in the $^{12}$C + $^{14}$C reaction should account for the parity dependence and the contribution of partial waves beyond the grazing one.

For the $^{12}$C + $^{14}$C system, the situation in the other weakly populated binary channels is less clear. Although structures are observed, the correlation with the above mentioned resonances is not evident. These channels require a complex rearrangement of nucleons. Thus, it is unlikely for them to be strongly coupled to any mode associated with the resonant behaviour.

#### *3.2.3.* The $^{14}$C + $^{16}$O reaction

For the $^{14}$C + $^{16}$O reaction, the excitation functions of the main reaction channels were measured using GRM by the Strasbourg group [14]. Broad resonances at $E_{\rm c.m.}$=19.5, 23, 27.5 and 31 MeV showed up quite strongly and were correlated in the $\gamma$-yields of the $^{18}$O(2$^+$) and (4$^+$) states (top-right panel of Fig. 3). The $^{12}$C + $^{18}$O binary exit channel corresponds to either an $\alpha$ or a $2n$ transfer mechanism. Weaker but correlated structure was also observed in the inelastic yields to the $^{14}$C(3$^-$) state. Again, this is remarkably similar to the resonances observed in the $\alpha$-type systems $^{16}$O + $^{16}$O and $^{12}$C + $^{16}$O studied previously using GRM [21, 25].

In the energy range in which the resonant structure was observed using GRM, the $^{14}$C + $^{16}$O reaction was also studied using KCM [17]. Angular distributions and excitation functions were measured at 17 different energies from $E_{\rm c.m.}$=21 MeV to 32 MeV. The remarkable and rather unique resonant behaviour of the $^{14}$C + $^{16}$O system is demonstrated in Fig. 5, which shows the angle integrated excitation functions of 5 different exit channels. Strongly correlated structures are observed in all channels at $E_{\rm c.m.}$=23, 27 and to a lesser extent at 31 MeV. The resonances appear at the same energies as in the GRM work [14] in which integrated cross sections were measured. Thus, these correlated structures observed in the integrated GRM and KCM yields of several binary channels are signatures of the molecular states in $^{30}$Si which decays with different partial widths into various C+O and $^{15}$N$+^{15}$N channels.

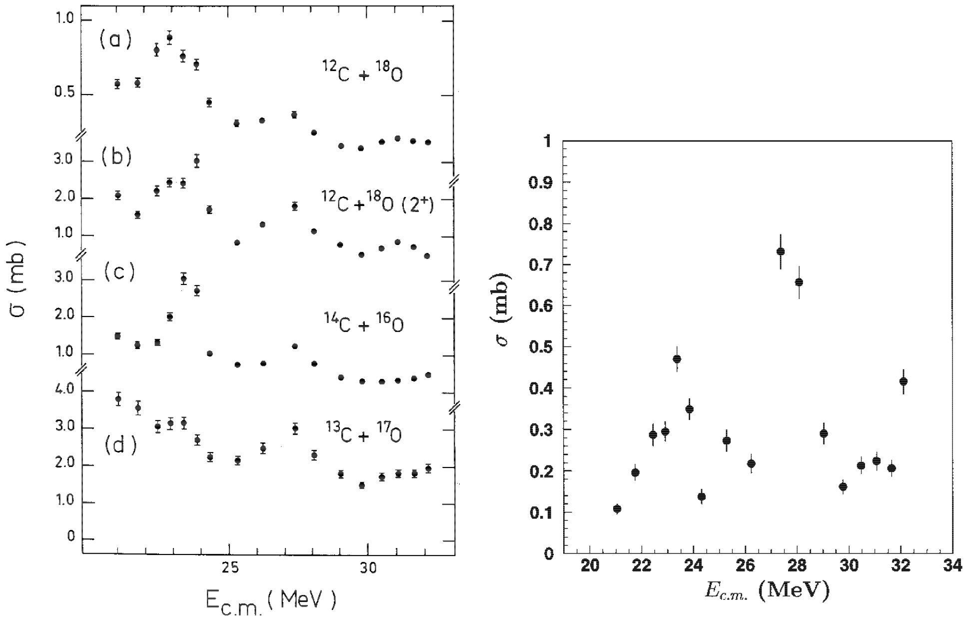


*Fig. 5. Excitation functions obtained using KCM for the following* $^{14}$C$+^{16}$O *reaction channels: a)* $^{12}$C$+^{18}$O, *b)* $^{12}$C $+^{18}$O(2$^{+}$), *c)* $^{14}$C$+^{16}$O, *d)* $^{13}$C$+^{17}$O *in the left panel and* $^{15}$N$+^{15}$N *in the right panel. In a), b) and d), the intensities were obtained by integrating the experimental angular distributions from 45° to 90°, while for c), the integration was performed from 90° to 120°. For the* $^{15}$N$+^{15}$N *channel, the* $\theta_{\rm c.m.} = 90°$ *excitation function is shown.*

It is interesting to scrutinize the evolution of the elastic angular distributions as a function of the incident energy displayed in Fig. 2 of Ref. [17]. These distributions evolve in a simple systematic way. They all have a maximum near 90°, and beyond 90° they do not change drastically displaying parallel ridges. As the energy increases, the changes occur at smaller forward angles: in a valley between two ridges, a new ridge (maximum) emerges. These new maxima appear at $E_{\rm c.m.}$ about 23, 27 and 31 MeV, namely at energies at which the correlated peaks are observed in the excitation functions. Obviously, the evolution of the elastic angular distributions is correlated with the resonant structure.

The angular distributions of the $^{12}$C$+^{18}$O channel show different behaviour at forward and at backward angles, which reflects the two different mechanisms, the $2n$-transfer and the $\alpha$-exchange process. The angular distribution of the most prominent resonance at 23 MeV was fitted with the relation $|\sum_L a_L P_L(cos\theta)|^2$. An acceptable fit was obtained, but at the expense of including 9 partial waves, $L = 0$

and all waves from $L$ =14 to 21 (for details on the fitting procedure and the choice of $L$-values see Ref. [28]). To reproduce the evolution of the angular distributions, new partial waves have to be added in the band of $L$-values as the energy increases. The above analysis does not rely upon any model. We merely stress the possibility that such angular distributions can be explained with a coherent band of partial waves. Structured angular distributions are caused by the beating of different $L$-values. Two important conclusions stem from the partial wave analysis: i) the needed partial waves have angular momenta which are larger than the grazing values and ii) the shape of the distributions can only be reproduced by including the low-$L$ partial waves. As in the $^{12}\mathrm{C}+^{14}\mathrm{C}$ case, the first of the above conclusions corroborates the picture of an extended configuration bound by the outermost nucleons as being the origin of the observed resonant structure.

The description of the shape of the on-resonance angular distributions requires more than one partial wave. The structure in the distributions are caused by the beating of neighbouring $L$-values. The dominant $L$, i.e. the spin of the resonance, can only be extracted from a phase-shift analysis of the angular distributions measured over a wide angular range, larger than in the experiments described in the present article. For the $^{14}\mathrm{C}+^{16}\mathrm{O}$ reaction, such an analysis is a particularly difficult task because it concerns four different exit channels ($^{14}\mathrm{C}+^{16}\mathrm{O}$, $^{12}\mathrm{C}+^{18}\mathrm{O}$, $^{13}\mathrm{C}+^{17}\mathrm{O}$ and $^{15}\mathrm{N}+^{15}\mathrm{N}$) which are all involved in the resonant process and which are strongly coupled.

## 4. $^{14}\mathrm{C}$ *induced reactions: refractive effects*

In the preceding section, we have demonstrated that all three low-energy $^{14}\mathrm{C}$-induced reactions $^{14}\mathrm{C}+^{14}\mathrm{C}$, $^{12}\mathrm{C}+^{14}\mathrm{C}$ and $^{14}\mathrm{C}+^{16}\mathrm{O}$ show strong resonant structures. This itself proves that for these reactions induced by a non $\alpha$-type nucleus, the absorption is weak as predicted by NOC and OCM. It is well known that in the $^{12}\mathrm{C}+^{12}\mathrm{C}$ collision, the text-book example of a weak absorption, when the incident energy increases above about 5 MeV per nucleon, the resonant structure evolves into refractive effects, nuclear rainbow and associated Airy oscillations [4, 15, 29]. The same features can be expected in the $^{14}\mathrm{C}$-induced reactions. As discussed above, the complex angular distributions measured for the $^{14}\mathrm{C}+^{16}\mathrm{O}$ reaction could only be explained by including a 'band' of $L$-values in the partial wave analysis [28]. Similarly to the nuclear rainbow phenomena, this is a signature of highly penetrating interior waves which are not completely absorbed and are required to fit the angular distributions.

For the $\alpha$-type systems $^{16}\mathrm{O}+^{16}\mathrm{O}$ and $^{16}\mathrm{O}+^{12}\mathrm{C}$, the refractive effects were studied at the Strasbourg Vivitron accelerator [28–32]. Detailed and large-angular-range elastic angular distributions were measured in the energy region just above the resonant region, i.e. between 5 and 10 MeV per nucleon. The elastic scattering angular distributions show not only the usual diffraction pattern, but also, at larger angles, refractive behaviour in the form of Airy structures. Together with the higher energy data reported for the same systems [34, 35], such systematic measurements of the elastic scattering resulted in the determination of a unique nucleus-nucleus potential. Indeed, it has been shown that the presence of the nuclear rainbow and the associated Airy structure in the elastic scattering reduces the ambiguities on the global character (shallow or deep) of the optical potential. The ensemble of measured data is very well described by the optical potential with a deep real part and a shallow imaginary part. The character of the imaginary part reflects the presence of incomplete absorption.

To predict what happens in the $^{14}$C-induced reactions, the obtained deeply attractive and weakly absorptive optical potentials were used to calculate the elastic angular distribution of the $^{14}\mathrm{C}+^{16}\mathrm{O}$ system at $E_{\mathrm{lab}}(^{16}\mathrm{O})$ =124 MeV. The results of this calculation are shown in Fig. 6. By using the potentials obtained by the fitting procedure of either the $^{16}\mathrm{O}+^{16}\mathrm{O}$ or $^{16}\mathrm{O}+^{12}\mathrm{C}$ scattering, the $^{14}\mathrm{C}+^{16}\mathrm{O}$ an-

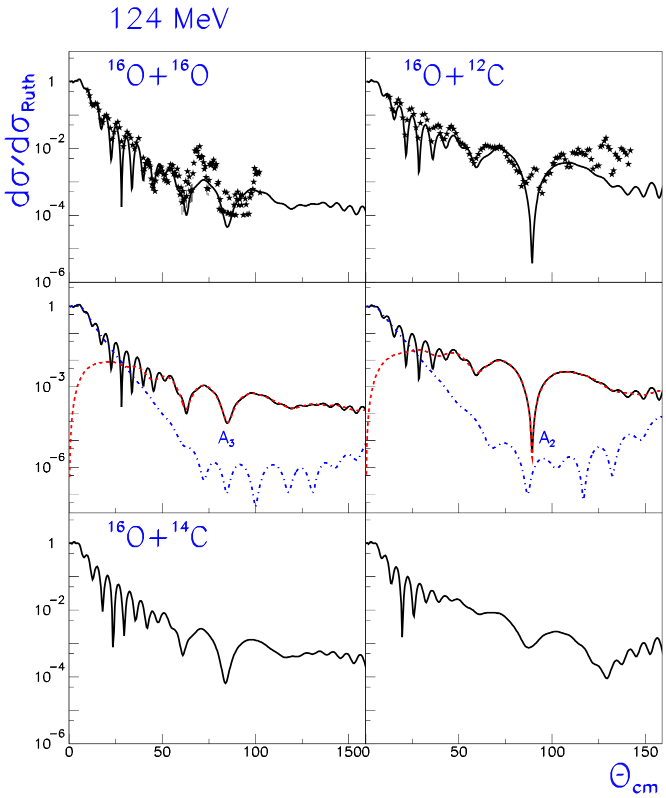


*Fig. 6. Measured elastic angular distributions of the* $^{16}\mathrm{O}+^{16}\mathrm{O}$ *(top-left panel) and* $^{16}\mathrm{O}+^{12}\mathrm{C}$ *(top-right panel) scattering at* $E_{\mathrm{lab}}$=*124* MeV, *together with the optical model fits (full curves) [29–31]. The middle panels show the nearside (dotted)–farside (dashed) decompositions of the above fits [28]. The Airy minima appearing in the distributions are labeled by* $A_2$ *(right) and* $A_3$ *(left), respectively. The bottom panels show the optical model predictions for the* $^{16}\mathrm{O}+^{14}\mathrm{C}$ *system using the optical model parameters obtained in the* $^{16}\mathrm{O}+^{16}\mathrm{O}$ *(left) and* $^{16}\mathrm{O}+^{12}\mathrm{C}$ *(right) fits.*

gular distributions have been calculated. Both distributions show a wide structure at large angles which have been interpreted as higher-order Airy minima. The predicted refractive behaviour of the $^{14}C+^{16}O$ system agrees with the preliminary results of a recent elastic scattering experiment [36]. Since the observability of both resonant and refractive phenomena is closely related to the degree of transparency of the nucleus-nucleus interaction, the appearance of refractive effects is also expected in the $^{12}C+^{14}C$ and $^{14}C+^{14}C$ systems, for which the resonant behaviour was demonstrated.

The ultimate goal of such studies is a unified description of refractive and resonant data with a strongly attractive nucleus-nucleus potential. Historically, the resonant data were explained by phenomenological optical potentials with shallow real and imaginary parts. It was stressed, however, that a shallow real potential was not able to reproduce the strength and positions of the gross structures appearing in the $\theta_{\mathrm{c.m.}} = 90^\circ$ cross sections of the $^{16}O+^{16}O$ elastic scattering as well as of those appearing in the $^{14}C+^{14}C$ scattering [18, 19, 41]. Compared with a realistic folding nucleus-nucleus potential, such shallow real potentials are essentially non-physical. Recently, some attempts have been made to fit the resonant data with the deep potentials obtained within refractive studies [37, 38]. It has been shown that such potentials are valid down to very low incident energy close to the Coulomb barrier. It is remarkable to notice that such deep potentials successfully describe both the bound and scattering states for the same system.

## 5. *The* $^{14}$C *radioactive beam*

The results reported in this article could not have been obtained without the use of radioactive $^{14}C$ beams and targets. The $^{14}C$ beam was produced using the negative-ion sources of the following tandem laboratories: Munich, Daresbury, Copenhagen, Orsay and Strasbourg in Europe, Los Alamos and Florida State University in the USA. Unfortunately, most of these facilities no longer exist, although the $^{14}C$ beams could reach 5 orders of magnitude stronger intensities than the typical beam-intensities delivered by other radioactive-beam facilities (for details on the production and handling of the $^{14}C$ beam see Ref. [11]). An accelerator delivering a $^{14}C$ beam of an energy up to 10 MeV per nucleon would be particularly useful not only for the study of refractive effects discussed in the present article, but also for the study of reactions involving highly neutron-rich light nuclei far from stability. Indeed, in the context of nuclear cluster physics, the $^{14}C$ beam would allow to induce multi-nucleon transfer reactions and thus give access to the spectroscopy of, e.g. neutron-rich Be, C and O isotopes, for which recent calculations predict the existence of very exotic states with a linear-chain-cluster structure composed of $\alpha$-particles and valence neutrons [39, 40].

## 6. *Conclusion*

It is very often stated in the literature that resonant structures in light heavy-ion collisions with the compound-nucleus mass less than $\sim$40 are exclusively observed in $\alpha$-type systems involving the $^{12}$C and $^{16}$O nuclei. The observation of di-nuclear molecular states depends on the spreading and escape widths of such states. Owing to the critical angular momentum for fusion, the escape width predominates at incident energies well above the Coulomb barrier. Therefore, the number of open reaction channels is most important. The NOC calculations show that for systems composed of tightly bound $\alpha$-type nuclei, there is a weak and surface transparent absorption which explains the observation of resonances in these systems and in particular in the $^{12}\text{C}+^{12}\text{C}$, $^{12}\text{C}+^{16}\text{O}$ and $^{16}\text{O}+^{16}\text{O}$ reactions. Moreover, NOC predicts that similar effects should be observed at energies well above the Coulomb barrier in reactions induced by the non $\alpha$-type nucleus $^{14}$C. The reason for that is the structure of $^{14}$C which has a closed neutron shell and semi-closed proton shell. Consequently, the first excited level is at high excitation energy ($E^* \approx 6.1$ MeV), while the structure of low-lying states is very similar to that of the closed-shell nucleus $^{16}$O.

In this paper, we have presented an overview of the results obtained by the Strasbourg–Zagreb collaboration in the search for resonant structures in the $^{14}$C-induced reactions $^{14}\text{C}+^{14}\text{C}$, $^{14}\text{C}+^{12}\text{C}$ and $^{14}\text{C}+^{16}\text{O}$. Excitation functions and angular distributions have been obtained for the main decay channels using two different but complementary experimental techniques. It turns out that all three systems show strong and correlated structures which are 'true' resonances and are observed mainly in the binary elastic, inelastic and transfer channels, i.e. channels which are particularly sensitive to the highest and close-to-grazing incident partial waves. All these observations are in good agreement with the NOC calculation which predicts a similarly weak and surface transparent absorption in the $^{14}$C and $^{16}$O induced reactions owing to the similarity of the low-energy spectra of these nuclei.

As the incident energy increases, the interaction time decreases and it has been shown recently that for the $\alpha$-type $^{12}\text{C}+^{12}\text{C}$, $^{12}\text{C}+^{16}\text{O}$ and $^{16}\text{O}+^{16}\text{O}$ systems the resonant behaviour evolves into a refractive feature with the formation of a nuclear rainbow and the associated Airy structures. It has been shown in the present article that such refractive features should also be observed in the above discussed reactions induced by $^{14}$C. There is a justified request for a $^{14}$C radioactive beam of an energy up to about 10 MeV per nucleon, not only to search for refractive effects, but also to perform a detailed spectroscopy of light neutron-rich $\alpha$-cluster nuclei. These cluster states will be ideally populated in multi-nucleon transfer reactions induced by $^{14}$C [39].

*Acknowledgements*

In this review article of the Strasbourg–Zagreb collaboration, we have mentioned experimental and theoretical works which involved a large number of physicists around the world. Their names can be found in the reference list and particularly in the works signed by one of the authors (F.H.). Here we would like to underline the exceptional contribution of Dr. R. M. Freeman who, before his retirement, took part in all aspects of this research programme. Special thanks are due to the tandem accelerator teams in Munich and Strasbourg who delivered the very precious $^{14}$C beams and also to R. Maier of the Munich target laboratory where the $^{14}$C pellets and targets were produced.

Nikola Cindro participated in some phases of the exposed research programme. His strong personality had a decisive influence on many physics decisions. Besides his contribution as a coworker in the above and a number of other joint Strasbourg–Zagreb experiments, his spiritual presence as a teacher and his inspiration did not fade with time. We share a feeling of an abiding sense of gratitude to him.

References

[1] E. Almquist, D. A. Bromley and J. A. Kuehner, Phys. Rev. Lett. **4** (1960) 515.

[2] B. Imanishi, Phys. Lett. B **27** (1968) 267; W. Scheid, W. Greiner and R. Lemmer, Phys. Rev. Lett. **25** (1970) 176; Y. Kondo, Y. Abe and T. Matuse, Phys. Rev. C **19** (1979) 1356; K. A. Erb and D. A. Bromley, Phys. Rev. C **23** (1981) 2781; N. Cindro and W. Greiner, J. Phys. G: Nucl. Phys. **9** (1983) L175; S. Marsh and W. D. M. Rae, Phys. Lett. B **180** (1986) 185.

[3] R. R. Betts and A. H. Wuosmaa, Rep. Prog. Phys. **60** (1997) 819; R. R. Betts, *Proc. 7$^{th}$ Int. Conf. Clustering Aspects of Nuclear Structure and Dynamics*, Rab, Croatia (1999), eds. M. Korolija, Z. Basrak and R. Čaplar, World Scientific, p. 109 and references therein.

[4] M. E. Brandan and G. R. Satchler, Phys. Rep. **285** (1997) 143 and references therein.

[5] N. Cindro and D. Počanić, J. Phys. G: Nucl. Phys. **6** (1980) 356; D. Počanić, *Ph. D. Thesis*, University of Zagreb, 1981; D. Počanić and N. Cindro, Nucl. Phys. A **433** (1985) 531.

[6] F. Haas and Y. Abe, Phys. Rev. Lett. **46** (1981) 1667.

[7] C. Beck, Y. Abe, N. Aissaoui, B. Djerroud and F. Haas, Phys. Rev. C **49** (1994) 2618.

[8] H. Feshbach, A. K. Kerman and R. H. Lemmer, Ann. Phys. **41** (1967) 230.

[9] W. Greiner and W. Scheid, J. Physique C **6** (1971) 91.

[10] N. Cindro, Ann. Phys. Fr. **13** (1988) 289.

[11] R. Maier, G. Korschinek, P. Spolaore, W. Kutschera, H. J. Maier and W. Goldstein, Nucl. Instr. Meth. **155** (1978) 55.

[12] R. M. Freeman, C. Beck, F. Haas, B. Heusch, H. Bohn, U. Kaüfl, K. A. Eberhard, H. Puchta, T. Senftleben and W. Trautmann, Phys. Rev. C **24** (1981) 2390.

[13] R. M. Freeman, F. Haas and G. Korschinek, Phys. Lett. B **90** (1980) 229.

[14] J. J. Kolata, C. Beck, R. M. Freeman, F. Haas and B. Heusch, Phys. Rev. C **23** (1981) 1056.

[15] A. Morsad, F. Haas, C. Beck and R. M. Freeman, Z. Phys. A **338** (1991) 61.

[16] R. M. Freeman, Z. Basrak, F. Haas, A. Hachem, G. A. Monnehan and M. Youlal, Phys. Rev. C **46** (1992) 589.

[17] R. M. Freeman, Z. Basrak, F. Haas, A. Hachem, G. A. Monnehan and M. Youlal, Z. Phys. A **341** (1992) 175.

[18] D. Konnerth, K. G. Bernhardt, K. A. Eberhard, R. Singh, A. Strzalkowski, W. Trautmann and W. Trombik, Phys. Rev. Lett. **45** (1980) 1154.

[19] D. M. Drake, M. Cates, N. Cindro, D. Počanić and E. Holub, Phys. Lett. B **98** (1981) 36.

[20] D. Konnerth, W. Trombik, K. G. Bernhardt, K. A. Eberhard, R. Singh, A. Strzalkowski and W. Trautmann, Nucl. Phys. A **436** (1985) 538.

[21] J. J. Kolata, R. C. Fuller, R. M. Freeman, F. Haas, B. Heusch and A. Gallmann, Phys. Rev. C **16** (1977) 891; J. J. Kolata, R. M. Freeman, F. Haas, B. Heusch and A. Gallmann, Phys. Rev. C **19** (1979) 2237.

[22] W. von Oertzen, H. G. Bohlen and M. Milin et al., Eur. Phys. J, in press.

[23] R. J. Peterson, H. C. Bhang, J. J. Hamill and T. G. Masterson, Nucl. Phys. A **425** (1984) 469.

[24] J. J. Kolata, R. M. Freeman, F. Haas, B. Heusch and A. Gallmann, Phys. Rev. C **21** (1980) 579.

[25] J. J. Kolata, R. M. Freeman, F. Haas, B. Heusch and A. Gallmann, Phys. Lett. B **65** (1976) 333; J. J. Kolata, R. M. Freeman, F. Haas, B. Heusch and A. Gallmann, Phys. Rev. C **19** (1979) 408.

[26] R. G. Stokstad, R. M. Wieland, G. R. Satchler, C. B. Fulmer, D. C. Hensley, S. Raman, L. D. Rickertsen, A. H. Snell and P. H. Stelson, Phys. Rev. C **20** (1979) 655.

[27] W. von Oertzen and H. G. Bohlen, Phys. Rep. **19** (1975) 1; D. Baye, Nucl. Phys. A **460** (1986) 581.

[28] R. M. Freeman, F. Haas, M. P. Nicoli, A. Morsad and Z. Basrak, Eur. Phys. J. A **4** (1999) 239.

[29] S. Szilner, *Ph. D. thesis*, Université Louis Pasteur, Strasbourg and University of Zagreb, 2001, IReS 01-03 Report.

[30] M. P. Nicoli, F. Haas, R. M. Freeman, N. Aissaoui, C. Beck, A. Elanique, R. Nouicer, A. Morsad, S. Szilner, Z. Basrak, M. E. Brandan and G. R. Satchler, Phys. Rev. C **60** (1999) 064608.

[31] M. P. Nicoli, F. Haas, R. M. Freeman, S. Szilner, Z. Basrak, A. Morsad, G. R. Satchler and M. E. Brandan, Phys. Rev. C **61** (2000) 034609.

[32] S. Szilner, M. P. Nicoli, Z. Basrak, R. M. Freeman, F. Haas, A. Morsad, M. E. Brandan and G. R. Satchler, Phys. Rev. C **64** (2001) 064614.

[33] M. P. Nicoli, *Thèse de Doctorat de l'Université Louis Pasteur*, Strasbourg, 1998, IReS 98-16 Report.

[34] E. Stiliaris, H. G. Bohlen, P. Fröbrich, B. Gebauer, D. Kolbert, W. von Oertzen, M. Wilpert and Th. Wilpert, Phys. Lett. B **223** (1989) 91; Dao T. Khoa, W. von Oertzen, H. G. Bohlen and F. Nuoffer, Nucl. Phys. A **672** (2000) 387.

[35] A. A. Ogloblin, Dao T. Khoa, Y. Kondō, Yu. A. Glukhov, A. S. Dem'yanova, M. V. Rozhkov, G. R. Satchler and S. A. Goncharov, Phys. Rev. C **57**, 1797 (1998); A. A. Ogloblin, Yu. A. Glukhov, W. H. Trzaska, A. S. Dem'yanova, S. A. Goncharov, R. Julin, S. V. Klebnikov, M. Mutterer, M. V. Rozhkov, V. P. Rudakov, G. P. Tiorin, Dao T. Khoa and G. R. Satchler, Phys. Rev. C **62** (2000) 044601.

[36] A. A. Ogloblin (private communication).

[37] C. Gao and Y. Kondō, Phys. Lett. B **408** (1997) 7.

[38] S. Ohkubo and K. Yamashita, Phys. Rev. C **66** (2002) 021301(R).

[39] M. Milin and W. von Oertzen, Eur. Phys. J. A **14** (2002) 295.

[40] N. Itagaki and S. Okabe, Phys. Rev. C **61** (2000) 044306; N. Itagaki, S. Okabe, K. Ikeda and I. Tanihata, Phys. Rev. C **64** (2001) 014301; N. Itagaki, S. Okabe, K. Ikeda and I. Tanihata, Eur. Phys. J. A **13** (2002) 43.

[41] M. E. Brandan and G. R. Satchler, Phys. Lett. B **256** (1991) 311.

## SLABA APSORPCIJA I REZONANCIJE U LAKIM TEŠKOIONSKIM REAKCIJAMA IZAZVANE JEZGROM $^{14}$C KOJA NEMA $\alpha$-PODSTRUKTURU

Opažanje rezonantnih struktura nuklearnih molekulskih konfiguracija u sustavima koji uključuju jezgre $^{12}$C i $^{16}$O, a koje imaju izrazitu grozdastu $\alpha$-podstrukturu, jasan su znak slabe i površinski prozirne apsorpcije u lakim teškoionskim reakcijama na energijama oko i znatno iznad Coulombove barijere. Takva slaba apsorpcija, tj. prozirnost nuklearne površine, predviđa se također za reakcije izazvane jezgrom $^{14}$C zbog posebne strukture niskoležećih stanja te jezgre, iako nije jezgra $\alpha$-tipa. U svjetlu pojava slabe apsorpcije, razmatramo eksperimentalno traženje rezonantnih struktura u reakcijama $^{14}$C + $^{14}$C, $^{14}$C + $^{12}$C i $^{14}$C + $^{16}$O, koje smo poduzeli u okviru suradnje grupa iz Strasbourga i Zagreba. Opažene su jake i korelirane rezonancije u sva tri proučavana sustava, a napose u onim izlaznim reakcijskim kanalima koji su osjetljivi na doprinos najviših parcijalnih valova ulaznog kanala reakcije. Porastom upadne energije, slaba i površinski prozirna apsorpcija uzrokuje refraktivne pojave, odnosno nuklearnu dugu. Doista, nuklearna duga je nedavno opažena u sustavima $\alpha$-tipa ($^{12}$C + $^{12}$C, $^{12}$C + $^{16}$O i $^{16}$O + $^{16}$O) za koje su na niskim energijama nađene izrazite nuklearne molekulske rezonancije. Predviđamo da će se takve refraktivne pojave opaziti na energijama iznad oko 5 MeV po nukleonu i za reakcije izazvane jezgrom $^{14}$C.